Ecological Applications, 0(0), 2021, e02388
© 2021 Ecological Society of America. This article has been contributed to by US Government employees and their work is in the public domain in the USA.

Assessing the robustness of time-to-event models for estimating unmarked wildlife abundance using remote cameras

KENNETH E. LOONAM,[1,6,8] PAUL M. LUKACS,[2] DAVID E. AUSBAND,[3,7]
MICHAEL S. MITCHELL,[4] AND HUGH S. ROBINSON[5]

[1]*Montana Cooperative Wildlife Research Unit, Wildlife Biology Program, W.A. Franke College of Forestry and Conservation, University of Montana, Natural Sciences Room 205, Missoula, Montana 59812 USA*
[2]*Wildlife Biology Program, W.A. Franke College of Forestry and Conservation, University of Montana, 32 Campus Drive, Missoula, Montana 59812 USA*
[3]*Idaho Department of Fish and Game, 2885 West Kathleen Avenue, Coeur d'Alene, Idaho 83815 USA*
[4]*U.S. Geological Survey, Montana Cooperative Wildlife Research Unit, Natural Sciences Room 205, University of Montana, Missoula, Montana 59812 USA*
[5]*Panthera and Wildlife Biology Program, W.A. Franke College of Forestry and Conservation, University of Montana, Natural Sciences Room 205, Missoula, Montana 59812 USA*

Citation: Loonam, K. E., P. M. Lukacs, D. E. Ausband, M. S. Mitchell, and H. S. Robinson. 2021. Assessing the robustness of time-to-event models for estimating unmarked wildlife abundance using remote cameras. Ecological Applications 00(00):e02388. 10.1002/eap.2388

Abstract. Recently developed methods, including time-to-event and space-to-event models, estimate the abundance of unmarked populations from encounter rates with camera trap arrays, addressing a gap in noninvasive wildlife monitoring. However, estimating abundance from encounter rates relies on assumptions that can be difficult to meet in the field, including random movement, population closure, and an accurate estimate of movement speed. Understanding how these models respond to violation of these assumptions will assist in making them more applicable in real-world settings. We used simulated walk models to test the effects of violating the assumptions of the time-to-event model under four scenarios: (1) incorrectly estimating movement speed, (2) violating closure, (3) individuals moving within simplified territories (i.e., movement restricted to partially overlapping circles), (4) and individuals clustering in preferred habitat. The time-to-event model was robust to closure violations, territoriality, and clustering when cameras were placed randomly. However, the model failed to estimate abundance accurately when movement speed was incorrectly estimated or cameras were placed nonrandomly with respect to habitat. We show that the time-to-event model can provide unbiased estimates of abundance when some assumptions that are commonly violated in wildlife studies are not met. Having a robust method for estimating the abundance of unmarked populations with remote cameras will allow practitioners to monitor a more diverse array of populations noninvasively. With the time-to-event model, placing cameras randomly with respect to animal movement and accurately estimating movement speed allows unbiased estimation of abundance. The model is robust to violating the other assumptions we tested.

Key words: abundance; camera trapping; density; estimation; monitoring; noninvasive; remote camera; sampling; space-to-event; time-to-event; unmarked.

INTRODUCTION

The use of remote cameras to monitor wildlife has seen extensive growth in recent decades, both in quantifying habitat use and in estimation of abundance and other demographic parameters. The first abundance estimates with remote cameras used capture–recapture methods and required species with naturally occurring marks that make individuals uniquely identifiable (Karanth 1995, Karanth and Nichols 1998). Mark–resight (Arnason et al. 1991) and spatial mark–resight (Sollmann et al. 2013*a*,*b*) models relax the uniquely identifiable requirement by allowing estimation of partially marked populations and populations with marked but not identifiable individuals. However, mark–resight models still require that some portion of the population be distinguishable, which is not the case for many populations of interest.

There are currently two broad approaches to estimating abundance of unmarked populations with remote cameras: estimating abundance directly by treating the

Manuscript received 16 June 2020; revised 4 January 2021; accepted 4 February 2021; final version received 18 May 2021. Corresponding Editor: Matthew G. Betts.

[6]Present address: Department of Fisheries and Wildlife, Oregon State University, Corvallis, Oregon USA

[7]Present address: U.S. Geological Survey, Idaho Cooperative Fish and Wildlife Research Unit, University of Idaho, 875 Perimeter Drive MS 1141, Moscow, Idaho 83844 USA

[8] E-mail: kenneth.loonam@oregonstate.edu

number of animals that appear on camera as a function of some set of detection parameters (such as detection probability or distance from an activity center) that is jointly estimated with abundance, as in the N-mixture (Royle 2004) and spatial count models (Chandler and Royle 2013); and estimating density within camera viewsheds that representatively sample a study area, including distance sampling (Howe et al. 2017), random encounter models (Rowcliffe et al. 2008), random encounter and staying time models (Nakashima et al. 2018), instantaneous sampling, and space- and time-to-event models (Moeller et al. 2018). The first set of models relies on potentially restrictive assumptions regarding the availability of individuals to be detected at a given camera. Meeting or checking these assumptions when individuals cannot be distinguished is challenging, and failing to meet the assumptions can cause bias in the estimates of abundance (Royle et al. 2013, Keever et al. 2017).

The second set of models relies on the broader assumption that cameras are placed randomly with respect to animal movement (i.e., that the cameras representatively sample the area to which inferences about density will be applied). This assumption can be met through random or systematic camera placement without any knowledge of animal movement patterns. Additional assumptions can increase the precision of models in this set at the cost of bias if the assumptions are not met (Moeller et al. 2018). In the least restrictive cases, such as instantaneous sampling and distance sampling, the number of animals on camera is treated as count data (Howe et al. 2017, Moeller et al. 2018). For low-density species, these models will be inefficient because most counts will be zero. An alternative is to model the encounter process between animals and randomly placed cameras as a function of density and movement speed. This approach requires information about movement speed, but has shown promise for both low-density species (Cusack et al. 2015, Loonam et al. 2020) and relatively abundant species (Rowcliffe et al. 2008, Moeller et al. 2018).

Time-to-event analysis, also called survival analysis and failure-time analysis, uses repeated measurements of the amount of time that elapses before an event of interest occurs to estimate the rate of that event. When estimating density from camera traps, the event of interest is an animal appearing in the viewshed, or a detection, and the rate of interest is density, or the number of animals per viewshed. To estimate density from repeated measures of the time until an animal appears in a viewshed, the model makes three additional assumptions.

First, the time-to-event model assumes that spatial counts of animals, or the number of animals in equal subsets of the landscape, are Poisson distributed at the scale of a camera viewshed. Ecologists commonly use the Poisson distribution to model count data (Thomas 1949). The spatial counts of animals will be Poisson distributed if individuals are equally likely to be in any section of a landscape and the location of one individual does not affect the location of other individuals. In field sampling, this assumption could be violated by animals grouping together, potentially due to clumped resources or social behavior, or by animals avoiding each other, potentially due to territoriality. Violating the Poisson-distributed assumption should bias the estimate low for aggregated populations and high for evenly dispersed populations. However, the model may be robust to some degree of aggregation or dispersion. Camera viewsheds sample a small area relative to animal space use, so, even when animals aggregate around a resource, most counts of animals in the viewshed will be 1 or 0 individuals, as expected under a Poisson distribution at low densities.

The second assumption of the time-to-event model is that of an accurate estimate of movement speed (including rest time) for the population. At constant density, encounter rate increases linearly with increasing animal movement speed, so any model that estimates density from encounter rate needs to account for movement speed (Carbone et al. 2001). In the time-to-event model, as movement speed increases, the observed time until an animal appears on camera will decrease, and the density estimate will be inflated. To account for this, we use animal movement speed and the area of camera viewsheds to define discrete time periods. We measure the time until an animal appears on camera as the number of those periods.

Third, the model assumes that the population is closed during sampling. Studies generally approximate closure by limiting sampling to a short period of time, but estimates of populations at low densities are more precise, with the additional data from longer sampling frames (Bischof et al. 2014, Dupont et al. 2019). In study designs that use an estimate of detection probability to estimate abundance, violating closure can bias the estimate of detection probability and subsequently abundance. The time-to-event model does not rely on an estimate of individual detection probability, so it handles lack of closure differently. If density changes during a survey through individuals leaving or joining the population, the time-to-event model should estimate the mean density through time, rather than the total number of individuals that were present for some portion of the survey (e.g., if the population drops from 20 individuals to 10 halfway through the study, the time-to-event model should estimate 15 individuals. However, if the population drops from 20 individuals to 10 at 4/5ths of the study period, the time-to-event model should estimate 18 individuals).

Most studies will fail to meet at least some of the assumptions of the model; therefore, before adopting these models more broadly, researchers need to understand the effects of violating assumptions on model performance (Gilbert et al. 2020). We used modified random walk models (Carbone et al. 2001, Codling et al. 2008) to test the effect of violating assumptions on the bias and precision of density estimates from the time-to-event model under eight scenarios. In each scenario, we modified a simple random walk model to test the effect of violating one of the model assumptions. In the first scenario, we looked at the effect of estimating the movement speed of the population inaccurately by changing how far individuals move in the simulation. In the second scenario, we allowed the length of each step to vary randomly, with the mean held constant. In the third scenario, we simulated different true abundances to test the effect of density on the estimate. In the fourth scenario, we varied how often individuals turn. In the fifth scenario, we tested the effect of violating the closure assumption by removing individuals during the simulation. In the sixth scenario, we tested the effect of animals being more evenly distributed than predicted by a Poisson distribution by restricting individual movement to partially overlapping areas representing territories. The final two scenarios tested the effect of violating the Poisson assumption and the random movement assumption by simulating movement with respect to a randomly generated habitat with two camera-placement strategies: random placement and cameras placed to target the preferred habitat. For both camera-placement methods in the habitat scenario, we applied two versions of the time-to-event model: the basic model and a second version that adjusts the density estimate for spatial variation in density using habitat covariates.

Materials and Methods

Time-to-event model

If the number of animals in camera viewsheds is Poisson distributed, the number of animals (N) that pass through the camera viewshed during a period of time is Poisson distributed around density (λ):

$$N \sim \mathrm{Pois}(\lambda). \qquad (1)$$

In time-to-event analysis, the time that passes until a Poisson-distributed event occurs (TTE) is exponentially distributed around the rate parameter (λ), in this case density:

$$\mathrm{TTE} \sim \mathrm{Exp}(\lambda). \qquad (2)$$

Because the time until a Poisson-distributed event occurs is exponentially distributed around density, we can estimate density with repeated measures of TTE.

Sampling for the time-to-event model requires definitions for two time intervals. First, the number of animals passing through the viewshed during a time period (N) depends on the length of the period. If the length of the period is equal to the amount of time the average animal takes to pass through a viewshed, N will be distributed around the mean number of animals per viewshed, or density (λ). Setting the length of the period requires an estimate of mean movement speed of the population (including rest time) and a measurement of the distance across the viewshed. Without accounting for movement speed, higher detection rates could be due to higher movement speed rather than higher density. Defining periods by the amount of time animals spend in a viewshed, on average, scales lambda to reflect the number of animals per viewshed while accounting for movement speed.

Second, sampling requires a defined occasion, or the amount of time spent observing the viewshed waiting for an event to occur. If an event does not occur during the sampling occasion, it is recorded as a right-censored event. Breaking the study into sampling occasions, rather than measuring the time between successive events, allows multiple measurements of TTE for each camera. It also eliminates the need to define a rule for independent events (e.g., Rowcliffe et al. [2008]), as only the first animal passing the camera during an occasion is counted. Defining the length of occasions as some number of periods (e.g., five periods per occasion) allows TTE to be recorded as the number of periods until an event occurs (e.g., if an animal appears on camera during the first period, TTE is 1 for that occasion; if an animals appears during the fifth period, TTE is 5). In practice, the number of periods in each occasion does not change the estimate or its precision (Loonam et al. 2020), and recording TTE as an integer number of periods, rather than a continuous time, causes a negligible bias (<1%, K. Loonam, *unpublished data*).

The time-to-event model can accommodate spatial variation in density. The basic application of the model estimates a single mean density across the sampled landscape; however, repeated measures of TTE for each camera allow for a density estimate at each camera. The variation in density among cameras can be modeled as the result of spatial covariates with a generalized linear model:

$$\log(\lambda_i) = \beta_0 + \boldsymbol{\beta X_i}, \qquad (3)$$

where λ_i is the estimated density at camera i and $\boldsymbol{\beta X_i}$ represents spatial covariates of camera i and their coefficients. With estimates for the effects of spatial covariates, the density of animals across the study area, $\bar{\lambda}$, can be estimated using

$$\bar{\lambda} = 1/n \times \sum_{i=1}^{n} \exp(\beta_0 + \boldsymbol{\beta X_i}), \qquad (4)$$

where n is the total number of potential camera locations in the study area, including unsampled locations, and X_i is the measure of the environmental covariates and potential camera location i.

Control

To test the effect of violating assumptions in each scenario, we compared each to a control simulation. In the control, 16 individuals moved randomly within a 100 × 100 unit square. Distance measurements do not have a defined unit in the simulation, so they can be thought of at any scale. However, whatever the units, the simulated density in terms of animals per viewshed is high compared to most studies (e.g., if the area of a viewshed is 50 m^2, the simulated density in the control would be 64 individuals per km^2). We divided the square into 36 cells with one detector, representing a camera trap with perfect detection, placed randomly in each cell. Detectors recorded an individual if the individual passed within a radius of $\pi/4$ units of a detector during a given step. We used a radius of $\pi/4$ units for the detectors so that the average path across the circular detection zone was 1 unit long (i.e., in 1 period, an individual takes 1 step, which is 1 unit long, allowing individuals to, on average, cross a detection zone in a single period given a random angle of approach; Appendix S1). The choice of circular detection zones is arbitrary. Because viewsheds vary in shape depending on the camera placement (Rowcliffe et al. 2008, Loonam et al. 2020), we use a shape that is easily simulated and measured.

Each individual took 1,000, 1-unit steps during the simulation, with turns at random angles every five steps. When a movement path would leave the 100 × 100 square, we flipped the *x*- or *y*-axis portion of that step and subsequent steps until the next turn to keep the individual in bounds. We defined periods as one step in the simulation, so recording the step at which a detection occurred also recorded TTE. We set occasion length equal to five periods. With 1,000 periods (defined by steps) and five periods per occasion, each run of the simulation was 200 occasions long with 16 individuals moving relative to 36 detectors for a total of 7,200 observations of TTE. We ran each simulation 1,000 times.

Movement speed

If animals moved faster than the estimated movement rate, we expected density to be overestimated, and vice versa. To simulate the effect of incorrectly estimating animal movement speed, we modified the step length while keeping the other variables constant. If step length equals 0.5, rather than 1, it will take individuals two steps to cross a detection zone. If step length equals 2, it will only take half a step to cross a detection zone. We used a range of 15 different step lengths (0.5, 0.6, 0.7, . . ., 1.4, 1.5) to capture the trend in abundance estimates from incorrectly estimating movement speed. We ran each speed simulation 1,000 times. As a post-hoc analysis, we fit a simple linear model between step length and estimated abundance to measure the magnitude of the effect.

Variable step length

Variable step lengths should not affect the abundance estimate as long as the mean movement speed is correctly estimated. To test this, we randomly drew step lengths from an exponential distribution with a mean of 1 ($\lambda = 1$). The resulting step lengths resemble an "L-shaped" curve with most steps being small but large values pulling the average up. This could be seen in a natural setting if animals tend to be relatively stationary then move long distances. We applied the same step length to each step taken between turns. Thus, if the step length was 2 and the number of steps taken between turns was 5, the individual would move 10 units, then turn and select a new step length.

Density

Higher densities should yield more precise estimates because higher encounter rates effectively provide more data. To test the effect of density on the time-to-event estimator, we assigned true abundance in the control simulation to powers of 2 from 2 to 256 (i.e., 2, 4, 8, . . ., 256).

Turn frequency

Turn frequency should not change the abundance estimate as long as individuals move through a detection zone, rather than turning within the detection zone. To vary turn frequency in the random walk, we modified the number of steps taken between each turn. In the control, individuals take five steps between turns. We ran the random walk with individuals taking from 1 to 25 steps between turns. Individuals always took the same number of steps between turns; there was no variation within runs.

Open population

If the closure assumption is violated and population is open, perhaps because of an extended survey period, we expected the time-to-event model to estimate mean density through time. To test the effect of violating the closure assumption, we simulated the population decreasing during the survey. We started with 20 individuals and censored individuals randomly throughout the survey until only 12 individuals remained. We censored individuals at random time steps, but, in each iteration of the simulation, the timing of the removals kept the average abundance equal to 16 individuals when the length of time each individual is present is taken into account.

Territoriality

To test the effect of animals being more evenly distributed than expected under the Poisson assumption, we simulated individuals moving in territories. We simulated simple territories by specifying the start location of each individual and restricting their movements in a radius around the start location. We arranged the 16 start locations in a grid, with the first individual starting at (x = 12.5; y = 12.5) and the last individual starting at (x = 87.5; y = 87.5). The nearest neighbors for each individual started 25 units away on the x- or y-axis. Individuals moved randomly within a radius of 12.5 units around their start location. When individuals left that radius, subsequent turn angles tended towards the individual's start location, with the strength of the effect increasing with distance. Those movement rules result in a circular area used by each individual with more time spent near the center of the "territory" and the edges overlapping with adjacent "territories." To check whether the territoriality model caused dispersion in the counts of individuals at cameras, we recorded the number of individuals that encountered each detector during each time step and compared that to the control simulation. We did not expect the "territories" to have any effect on the time-to-event model, because, even with completely random movement, most cameras only have one animal in the viewshed at a given time.

Habitat—random cameras

For the two scenarios testing the effect of animals clustering in high-quality habitat, we modeled individuals to move preferentially toward high-quality habitat on a simulated landscape. To generate the landscape, we drew random habitat quality scores from a normal distribution at two levels of hierarchy, 16 large cells each divided into 625 subcells. The first level of hierarchy divided the landscape into a 4 × 4 grid, with the mean habitat quality score for each of the 16 cells drawn from a standard normal distribution. The second level of hierarchy provided habitat values for each subcell drawn from a normal distribution centered on the mean value of the habitat quality score of the cell. The resulting landscape consists of 16 cells, each 25 × 25 subcells, with habitat quality scores that tend to be more similar within cells than between cells (Fig. 1).

We used a simplistic model of animal movement relative to habitat to simulate preference for higher habitat quality scores. For each new angle an individual selected, we averaged the habitat scores along eight potential paths, the paths that go in a cardinal direction and the paths halfway between any two cardinal directions. We generated the actual turn angle from a circular distribution centered on the direction with the highest average habitat quality score. Randomly drawing the direction of travel results in individuals tending toward the best adjacent habitat with the variance allowing occasional movements away from the best habitat to prevent individuals from getting stuck in one part of the landscape (Fig. 1).

We fit the basic time-to-event model in which mean density is estimated directly from the observed TTE (Eq. 2) and the model estimating density by adjusting for habitat with a generalized linear model (Eqs. 3, 4). Similar to the territory model, we recorded the number of individuals encountering each detector during a time step to compare the dispersion in counts to the control. We also recorded the number of points in each subcell and the habitat score of the subcells. We fit a negative binomial GLM between the counts in each subcell and

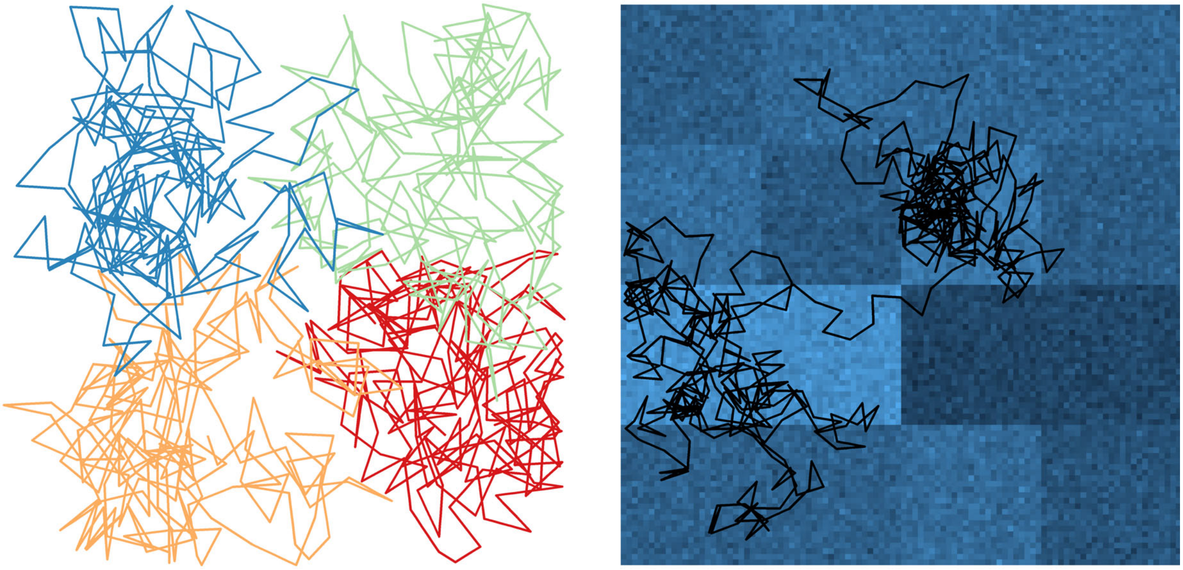

FIG. 1. Two simulated paths from the modified random walks. The left figure shows four individuals moving in simulated territories with the bottom and left sides bounding the simulated area. The figure on the right is an individual moving on a landscape to test the effect of clustered movements on the time-to-event model. Light colors represent preferred habitat. The individual tends toward preferred habitat and avoids less-preferred habitat, resulting in clustered movement.

the habitat score to examine the actual effect of the simulated habitat preference, which, because of the stochastic simulation, was not known in advance. We chose a negative binomial model because we expected the variance between counts to be greater than the mean count, and we did not want to inflate our power to detect an effect. In the randomly placed camera scenario, we expected both the basic model and the version adjusting for spatial variation in density to estimate density accurately.

Habitat—targeted cameras

To test the effect of nonrandom movement with respect to the cameras, we placed cameras nonrandomly with respect to the simulated landscape. The simulations of targeted camera placement use the same habitat generation and habitat preference rules as the habitat simulations with random camera placement. In all of the previous simulations, we placed one camera randomly in each of 36 sampling cells. In the targeted camera placement simulation, we assigned each camera to the subcell with the single highest habitat quality score in each sampling cell. This targeted sampling maximized detections, as might be the goal in capture–recapture or occupancy studies. However, for time-to-event studies, sampling to maximize detections will inflate the density estimate by lowering the observed TTE. Again, we estimated density twice for each run of the simulation, once without adjusting for habitat, and once adjusting for habitat with the generalized linear model (GLM). With targeted camera placement, we expected the basic model to overestimate density and the version adjusting for spatial variation in density to counteract the bias caused by targeted camera placement.

Statistical methods

We used Bayesian methods to estimate abundance from each run of the simulations using Markov chain Monte Carlo (MCMC) implemented in JAGS (Plummer 2017) through R (R Development Core Team 2019) and the R2jags package (Su and Yajima 2015). We could not assess model convergence for each run of the simulations individually, so we ran each model for a burn-in of 10,000 iterations then updated the model in batches of 100,000 iterations of three chains until the Gelman–Rubin convergence diagnostic ($\hat{R}$) (Gelman and Rubin 1992) was <1.1. We discarded any simulations that failed to achieve an $\hat{R}$ value <1.1 within 500,000 iterations. The posterior distributions of the initial runs were symmetrical, so we recorded the mean of the posterior as the estimate of abundance and the standard deviation (SD) of the posterior as a measure of precision to save computing memory during the simulation runs.

We examined the bias and the precision of the estimator for each simulation scenario. We used relative bias (RB) to measure bias

$$\mathrm{RB} = 1/n \sum_{j=1}^{n} (E_j - A)/A, \tag{5}$$

where n is the total number of runs of the simulation, E_j is the estimated abundance on the jth run of the simulation, and A is the true abundance. We examined two versions of precision: the observed precision (how precise the point estimates of abundance were between runs) and the estimated precision (how precise the model estimate was for each run). We used SD of the estimated abundances from each scenario to examine the observed precision:

$$\mathrm{SD} = \sqrt{1/n - 1 \sum_{j=1}^{n} \left(\left(E_j - \overline{E} \right)^2 \right)}, \tag{6}$$

where n is the total number of runs of the simulations, E_j is the estimated abundance on the jth run of the simulation, and $\overline{E}$ is the mean of the estimates of abundance. To examine the estimated precision, we took the SD of the poster distribution for each run of the simulation and recorded the mean of those SDs as the estimated precision. We compared the observed and estimated SD to check the accuracy of the precision estimates from the time-to-event model. We also report coverage, the proportion of runs in which the 95% credible interval contained the true abundance.

RESULTS

Control

In the control simulation, the time-to-event model estimated a mean of 15.45 (Table 1) animals, slightly below truth (N = 16 individuals). The observed SD of the estimates was 1.96, and the mean estimated SD was 1.49, meaning that the model overestimated precision. Precision was overestimated in almost all of the simulations. Coverage in the control simulation was 0.85, slightly below expected value of 0.95. Throughout this section we summarize the results of each simulation and draw attention to places where each simulation deviates from the control. The full results are presented in Table 1 or visualized in Fig. 2.

Speed

Incorrectly estimating speed had a linear effect on abundance estimates in the simulation (Fig. 2a). At the low end of the tested speeds (step length = 0.5), $\overline{x}$ abundance was 9.20 (SD = 2.16). At the high end of the tested speeds (step length = 2) the $\overline{x}$ abundance estimate was 28.36 (SD = 2.29) (Table 1). The relationship between step length and estimated abundance was linear with a coefficient of 0.80 (SE = 0.002; Fig. 2a).

TABLE 1. Results from simulations testing the effects of violating the assumptions of the time-to-event model on abundance estimates.

Simulation	Mean of estimates	SD of estimates	Mean SD	% Bias	Coverage
Control	15.45	1.96	1.49	−3.46%	0.85
Speed = 0.5	9.20	2.16	1.23	−42.5%	0.04
Speed = 2	28.36	2.28	2.17	77.2%	0.00
Open population	15.41	1.96	1.49	−3.67%	0.84
Territoriality	15.37	2.10	1.49	−3.88%	0.80
Variable step length	15.71	1.96	1.50	−1.81%	0.87
Habitat—Random—Base	16.34	2.70	1.53	2.14%	0.73
Habitat—Random—GLM	16.14	2.52	2.41	0.84%	0.91
Habitat—Targeted—Base	26.52	3.36	1.96	65.8%	0.01
Habitat—Targeted—GLM	11.86	4.64	4.18	−25.9%	0.68

Notes: Mean estimate is the mean of the reported abundance estimates from each iteration of the simulation. SD of estimates is the observed precision as measured by the SD of the estimates of abundance from each run. Mean SD is the estimated precision as measured by the mean of the SDs of the posterior distribution of each run. Bias is measured as the percent bias.

(a) Movement speed

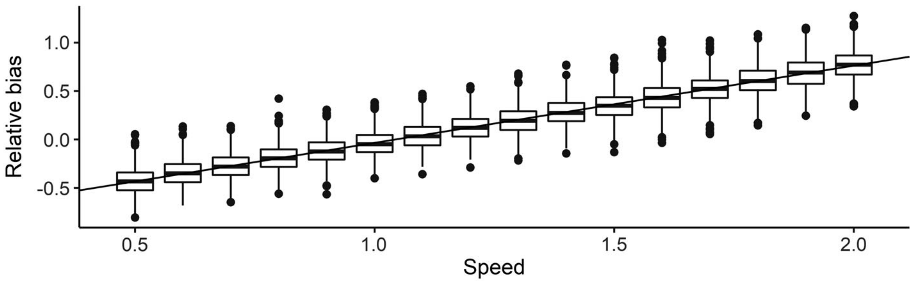

(b) Changing density

(c) Turn frequency

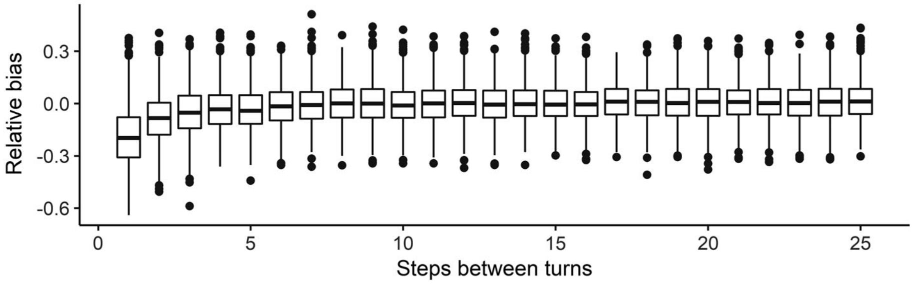

FIG. 2. Box plots of bias in abundance estimates from random walk models testing the effect of three variables on the time-to-event model. (a) Box plots of bias caused by varying movement on the distance traveled during each step (from 0.5 to 2) while holding estimated step length at 1. The line is the linear model of step length vs bias. The slope is 0.80. (b) Box plots of the bias in estimates of abundance from the time-to-event model when abundance varied from 2 to 256 individuals. (c) Box plots of bias in abundance estimates at variable turn frequencies. The number of steps taken before a new, random travel angle was taken varied from 1 to 25. At approximately three steps between turns, the bias remains stable near 0 up to 25 steps between turns.

Variable step length

Allowing step length to vary according to an exponential distribution did not affect the abundance estimates. The mean estimated abundance was 15.71 (SD = 1.50). Having variable step length did not lead to different results from the control, indicating that mean movement speed is sufficient for the time-to-event model.

Density

Varying density did not cause bias in the estimate of abundance (Fig. 2b). As expected, higher densities resulted in higher precision; however, the gap between the observed and estimated precision increased at true abundances higher than 16. From 2 individuals to 16 individuals, coverage was between 0.82 and 0.83. At 32 individuals coverage fell to 0.80, and by 256 individuals coverage was 0.62, indicating that, at very high densities, precision might be overestimated.

Turn frequency

High turn frequencies caused a negative bias in the abundance estimates with 1 and 2 steps between turns resulting in estimates of abundance biased low (Fig. 2c). At 3 steps between turns and higher, there was no noticeable bias.

Open population

In our simulation testing the effect of violating closure, the time-to-event model estimated the mean abundance as 15.41 individuals (SD = 1.96) (Table 1), approximating the control simulation (Appendix S2: Fig. S3b). This result supports the prediction that the time-to-event model estimates the average abundance through time when density changes during the course of a survey.

Territoriality

Simulations that restricted individuals to “territories” resembled the control simulation. The estimated abundance from the territorial simulation was 15.37 individuals (SD = 2.10; Table 1). The count of animals at each camera during each occasion closely resembled the control (means of 0.029 and 0.028 for the territory and control simulations), as did the SD of counts (means of 5.20 and 4.82, respectively) indicating that the territories did not cause underdispersion relative to the control.

Habitat—random cameras

In simulations where individuals had habitat preferences, but where cameras were still placed randomly, the estimates remained in the same general range as the control. The model with no adjustment for spatial variation in density returned a mean estimate of 16.34 individuals (SD = 2.70), whereas the model using the GLM to adjust for habitat returned a mean estimate of 16.14 individuals (SD = 2.52) (Table 1). The negative binomial GLM fit to the count of individuals passing through each habitat pixel showed a positive effect of habitat in every run of the simulation with $\overline{\beta} = 0.24$ (SD = 0.054) and $\overline{se} = 0.0047$. The time-to-event GLM detected the positive effect in the 95% CRI 92% of the time. This shows that the simulation successfully created a positive relationship between habitat and frequency of use and that the GLM in the time-to-event model was able to detect a relationship between density and habitat nearly as often as expected.

Habitat—targeted camera placement

In simulations with targeted camera placement designed to maximize detections, both the basic model and the model using a GLM to adjust for habitat failed to estimate abundance accurately. The basic model overestimated abundance (mean $N = 26.52$; SD = 3.36), and the GLM-adjusted model underestimated abundance (mean $N = 11.86$; SD = 4.64). In the targeted camera placement scenario, the GLM detected a positive relationship between λ and habitat in the 95% CRI 86% of the time.

Neither of the habitat simulations resulted in counts that were convincingly overdispersed relative to the control (Appendix S2; Fig. S4). Both showed a higher variance in counts among cameras (mean SD of 5.20 for the control, 7.67 for random placement, and 10.60 for targeted placement), which should be expected because some cameras will fall in high-quality habitat and others in low-quality habitat. However, the SD of count·camera^{-1}·occasion^{-1}, which includes both spatial and temporal variation in counts, was comparable between the control and random placement simulations (mean of 0.25 for the control and 0.24 for the random placement). The SD of count·camera^{-1}·occasion^{-1} was higher in the targeted camera placement simulation (0.31) than in the control, but that can be explained by the higher mean count per occasion of the targeted placement simulation (0.028 for the control and 0.047 for targeted placement). Because the dispersion was not convincingly different from the control, the habitat simulations are better thought of as a violation of perfect random movement than as a violation of the Poisson assumption.

DISCUSSION

Our simulations show that the time-to-event model is robust to many scenarios commonly encountered in studies of wild populations that violate the model’s assumptions. Neither territoriality of a species, nor open populations bias the results, and when animals move nonrandomly with respect to habitat, the model is unbiased as long as cameras are placed randomly. However, both targeting high-quality habitat when placing cameras and incorrectly estimating movement speed bias the estimate of abundance.

Incorrectly estimating speed caused a linear bias in the abundance estimate (Fig. 2) with overestimates of speed causing under estimation of abundance and vice versa. The model requires movement speed to estimate how long an individual will spend in a viewshed on average, which would be best provided by relatively fine-scale data such as short fix interval GPS (global positioning system) collar data from the population being sampled. If collar data are unavailable, sufficient estimates of movement speed may exist in the literature, particularly for well-studied species. Additionally, with the appropriate camera setup, practitioners can estimate movement speed directly from the camera data (Rowcliffe et al. 2016, Nakashima et al. 2018). This could be particularly useful for camera studies, as both the time-to-event model and unbiased estimates of movement speed from cameras rely on random camera placement. If movement data are unavailable or unreliable, the space-to-event model may be more applicable but will be less precise (Moeller et al. 2018). Because of similarity in their assumptions and approach to estimating abundance, we expect the space-to-event model to respond similarly to the time-to-event model when assumptions are violated.

High turn frequencies caused a negative bias in abundance estimates. The length of the period should be defined as the amount of time an average animal spends in the viewshed. If animals turn within the viewshed or immediately re-enter the viewshed, that length of time will be longer than calculated by dividing distance by speed. If animal movement is measured as relatively linear on the scale of viewsheds, turn frequency should not cause bias. In practice, this will not be a problem with estimates from GPS collars, where the fix intervals will miss extremely fine scale movement, or with estimates from cameras, where practitioners can measure the time spent in the viewshed directly (Nakashima et al. 2018).

Simulating high densities inflated the precision of the estimates, however, the densities we simulated are higher than most of the densities in real-world applications. For example, in the runs with 32 individuals, which is when coverage of the CRI began to decline, if the area of the detection zones was 50 m^2 (the area of a 45° wedge with an 8-m detection radius, comparable to common study designs; see Rowcliffe et al. 2008 and Loonam et al. 2020), the simulated density would have been equivalent to 64 individuals•km^{-2}. High densities could interact with other factors, such as territoriality or clumping in high quality habitat, to cause overdispersion or underdispersion. However, the mean number of animals per viewshed (λ) will still be much <1, even in high-quality habitat. Social behavior, such as traveling in groups, could cause overdispersion of counts. The extent to which that would impact the time-to-event model likely depends on how tightly the animals group relative to the size of the viewshed. If social grouping does cause bias, adjusting for it with an independent measure of group size, similar to the random encounter model (Rowcliffe et al. 2008), could adjust for the bias.

The open population simulation shows that the model handles closure differently than capture–recapture models. Capture–recapture methods rely on estimating the probability of detecting individuals to estimate abundance (N) with

$$\hat{N} = \frac{C}{\hat{p}},$$

where C is the observed count of animals and $\hat{p}$ is the estimated detection probability (Nichols 1992). When individuals are present and available to be detected during one portion of a survey, but not another, detection probability is underestimated and abundance is overestimated, approximating the total number of animals that were in the study area during some portion of the survey or decreasing precision (Kendall 1999). In contrast, the time-to-event model estimates the mean density through time. This means that lack of closure does not bias the estimate or decreases the precision in the same way it does in capture–recapture studies, potentially allowing sampling over a longer time frame. If the change in abundance through time is of interest, practitioners can break the survey into multiple periods and estimate the average abundance in each period at the cost of some precision.

In the habitat simulations with randomly placed cameras, both the base model and the model adjusting for habitat with a GLM returned estimates comparable to the control simulation, indicating that nonrandom movement does not bias the model as long as cameras are placed randomly. The most significant difference between the base model and the GLM model was precision. Both models were less precise than the control simulation, but the GLM model had the most accurate estimate of precision. This could be due to accurately estimating the effect of habitat on density or to adding an additional variable. Any additional variable will increase the width of the CRI.

Nonrandom sampling biases estimators (Fisher 1925). In the time-to-event model, targeting landscape features to maximize detections (e.g., roads and trails) will likely be the most common form of nonrandom sampling. In our habitat simulations with targeted camera placement, the base time-to-event model greatly overestimated abundance (27 vs. 16), and the time-to-event model with a GLM adjusting for habitat greatly underestimated abundance (12 vs. 16). The underestimation of the GLM adjusted model may be caused by a nonlinear effect of habitat. With the targeted camera placement, lower-quality habitats were not sampled. If the relationship between density and habitat quality is different at the high and low ends of the habitat values, extrapolating to the unsampled range of habitat values will fail. Further work could explore alternative sampling strategies that might provide unbiased estimates while still improving detection rates, such as targeting the best habitat with a portion of the cameras while placing the rest of the cameras randomly to sample the full range of habitat quality. However, monitoring a random sample of habitat by deploying cameras at randomly or systematically generated points, rather than sampling to maximize detections, remains the most reliable sampling technique for minimizing bias. Low detection rates of randomly placed cameras could be countered by extended camera deployments or deploying additional cameras. Data from surveys with camera placement that was not designed to sample the landscape randomly are unlikely to provide unbiased estimates from the time-to-event model.

One assumption of the time-to-event model that we did not test here is perfect detection of animals within the viewshed. False negatives are guaranteed in almost any study relying on motion-triggered cameras. Estimating the rate of false negatives, potentially through a dual-camera setup, distance sampling (Howe et al. 2017), or walk tests, allows its inclusion in the likelihood (Moeller et al. 2018).

We encourage further research on the effects of violating assumptions on all of the methods for estimating abundance of unmarked populations with remote cameras. Most papers that use these methods do not include discussions of the model assumptions and how well they are met (Gilbert et al. 2020). We expect methods that are similar to the time-to-event model, such as the space-to-event (Moeller et al. 2018) and random encounter (Rowcliffe et al. 2008) models, to perform similarly to the time-to-event model when assumptions are violated, though the space-to-event model should be unaffected by animal movement speed. Additionally, methods that focus on sampling the landscape have assumptions that are easier to meet than methods that attempt to estimate abundance by sampling unmarked individuals. Placing cameras randomly to representatively sample a landscape does not require any knowledge of animal movement or distribution relative to the sampling grid. Exploring all of the methods with similar, simulation-based approaches will help compare the methods and understand their utility.

Acknowledgments

Any use of trade, firm, or product names is for descriptive purposes only and does not imply endorsement by the U.S. Government. Funding and support for this project were provided by Idaho Department of Fish and Game, the Federal Aid in Wildlife Restoration Act, the Montana Cooperative Wildlife Research Unit, and the Wildlife Biology Program at the University of Montana. W. M. Joel helped us find our second wind whenever the simulations reminded us that we are only human. Two anonymous reviewers and Dr. Matthew Betts (Content Matter Editor) provided invaluable feedback they helped expand and improve this manuscript. All authors contributed to the conception and design of this project. KL coded the simulations and conducted the analysis. PL assisted with interpretation of the results. KL and HR wrote the paper. PL, DA, and MM provided critical revisions for the paper. All authors approved the final version to be published.

Literature Cited

Arnason, A. N., C. J. Schwarz, and J. M. Gerrard. 1991. Estimating closed population size and number of marked animals from sighting data. Journal of Wildlife Management 55:716–730.

Bischof, R., S. Hameed, H. Ali, M. Kabir, M. Younas, K. A. Shah, J. U. Din, and M. A. Nawaz. 2014. Using time-to-event analysis to complement hierarchical methods when assessing determinants of photographic detectability during camera trapping. Methods in Ecology and Evolution 5:44–53.

Carbone, C., et al. 2001. The use of photographic rates to estimate densities of tigers and other cryptic mammals. Animal Conservation 4:75–79.

Chandler, R. B., and J. A. Royle. 2013. Spatially explicit models for inference about density in unmarked or partially marked populations. Annals of Applied Statistics 7:936–954.

Codling, E. A., M. J. Plank, and S. Benhamou. 2008. Random walk models in biology. Journal of the Royal Society Interface 5:813–834.

Cusack, J. J., A. Swanson, T. Coulson, C. Packer, C. Carbone, A. J. Dickman, M. Kosmala, C. Lintott, and J. M. Rowcliffe. 2015. Applying a random encounter model to estimate lion density from camera traps in Serengeti National Park, Tanzania. Journal of Wildlife Management 79:1014–1021.

Dupont, P., C. Milleret, O. Gimenez, and R. Bischof. 2019. Population closure and the bias-precision trade-off in spatial capture–recapture. Methods in Ecology and Evolution 10:661–672.

Fisher, R. A. 1925. Theory of statistical estimation. Mathematical Proceedings of the Cambridge Philosophical Society 22:700–725.

Gelman, A., and D. B. Rubin. 1992. Inference from iterative simulation using multiple sequences. Statistical Science 7:457–511.

Gilbert, N., J. Clare, J. Stenglein, and B. Zuckerberg. 2020. Abundance estimation with camera traps. Conservation Biology 35:88–100.

Howe, E. J., S. T. Buckland, M.-L. Després-Einspenner, and H. S. Kühl. 2017. Distance sampling with camera traps. Methods in Ecology and Evolution 8:1558–1565.

Karanth, K. U. 1995. Estimating tiger *Panthera tigris* populations from camera-trap data using capture–recapture models. Biological Conservation 71:333–338.

Karanth, K. U., and J. D. Nichols. 1998. Estimation of tiger densities in India using photographic captures and recaptures. Ecology 79:2852–2862.

Keever, A. C., C. P. McGowan, S. S. Ditchkoff, P. K. Acker, J. B. Grand, and C. H. Newbolt. 2017. Efficacy of N-mixture models for surveying and monitoring white-tailed deer populations. Mammal Research 62:413–422.

Kendall, W. L. 1999. Robustness of closed capture–recapture methods to violations of the closure assumption. Ecology 80:2517–2525.

Loonam, K. 2021. keloonam/Loonam_et_al_2021_Walk_Models: Release for Eco Apps paper (Version v1.0.0). Zenodo. https://doi.org/10.5281/zenodo.4771037

Loonam, K. E., D. E. Ausband, P. M. Lukacs, M. S. Mitchell, and H. S. Robinson. 2020. Estimating abundance of an unmarked, low-density species using cameras. Journal of Wildlife Management 85:87–96.

Moeller, A. K., P. M. Lukacs, and J. S. Horne. 2018. Three novel methods to estimate abundance of unmarked animals using remote cameras. Ecosphere 9:e02331.

Nakashima, Y., K. Fukasawa, and H. Samejima. 2018. Estimating animal density without individual recognition using information derivable exclusively from camera traps. Journal of Applied Ecology 55:735–744.

Nichols, J. D. 1992. Capture–recapture models. BioScience 42:94–102.

Plummer, M. 2017. JAGS: Just Another Gibbs Sampler. https://mcmc-jags.sourceforge.io/

R Development Core Team. 2019. R: a language and environment for statistical computing. R Foundation for Statistical Computing, Vienna, Austria. www.r-project.org

Rowcliffe, J. M., J. Field, S. T. Turvey, and C. Carbone. 2008. Estimating animal density using camera traps without the need for individual recognition. Journal of Applied Ecology 45:1228–1236.

Rowcliffe, J. M., P. A. Jansen, R. Kays, B. Kranstauber, and C. Carbone. 2016. Wildlife speed cameras: measuring animal travel speed and day range using camera traps. Remote Sensing in Ecology and Conservation 2:84–94.

Royle, J. A. 2004. N-mixture models for estimating population size from spatially replicated counts. Biometrics 60:108–115.

Royle, J. A., R. B. Chandler, C. C. Sun, and A. K. Fuller. 2013. Integrating resource selection information with spatial capture–recapture. Methods in Ecology and Evolution 4:520–530.

Sollmann, R., B. Gardner, R. B. Chandler, D. B. Shindle, D. P. Onorato, J. A. Royle, and A. F. O'Connell. 2013*a*. Using multiple data sources provides density estimates for endangered Florida panther. Journal of Applied Ecology 50:961–968.

Sollmann, R., B. Gardner, A. W. Parsons, J. J. Stocking, B. T. Mcclintock, T. R. Simons, K. H. Pollock, and A. F. O'Connell. 2013*b*. A spatial mark–resight model augmented with telemetry data. Ecology 94:553–559.

Su, Y.-S., and M. Yajima. 2015. R2jags. https://cran.r-project.org/web/packages/R2jags/index.html

Thomas, M. 1949. A generalization of Poisson's binomial limit for use in ecology. Biometrika 36:18–25.

Supporting Information

Additional supporting information may be found online at: http://onlinelibrary.wiley.com/doi/10.1002/eap.2388/full

Open Research

Code for the simulations (Loonam 2021), which produced all data presented here, are available on Zenodo: http://doi.org/10.5281/zenodo.4771037